Specificity of Human Aldo-Keto Reductases, NAD(P)H:Quinone Oxidoreductase, and Carbonyl Reductases to Redox-Cycle Polycyclic Aromatic Hydrocarbon Diones and 4-Hydroxyequilenin-o-qu...

ARTICLE *in* CHEMICAL RESEARCH IN TOXICOLOGY · SEPTEMBER 2011

Impact Factor: 3.53 · DOI: 10.1021/tx200294c · Source: PubMed

Published in final edited form as:
Chem Res Toxicol. 2011 December 19; 24(12): 2153–2166. doi:10.1021/tx200294c.

Specificity of Human Aldo-Keto Reductases, NAD(P)H: Quinone Oxidoreductase and Carbonyl Reductases to Redox-Cycle Polycyclic Aromatic Hydrocarbon Diones and 4-Hydroxyequilenin-*o*-Quinone

Carol A. Shultz[†], **Amy M. Quinn**[‡], **Jong-Heum Park**[‡], **Ronald G. Harvey**[*], **Judy L Bolton**[**], **Edmund Maser**[**], and **Trevor M. Penning**[‡,⊥]

[†]Department of Biochemistry and Biophysics, Perelman School of Medicine, University of Pennsylvania, Philadelphia, Pennsylvania 19104

[‡]Center of Excellence in Environmental Toxicology, Department of Pharmacology, Perelman School of Medicine University of Pennsylvania, Philadelphia, Pennsylvania 19104

[*]The Ben May Department of Cancer Research, University of Chicago, IL 60637

[**]Department of Medicinal Chemistry and Pharmacognosy, College of Pharmacy, University of Illinois, Chicago, IL 60612

[***]Institute of Toxicology and Pharmacology for Natural Scientists, University Medical School Schleswig-Holstein, Kiel, Germany

Abstract

Polycyclic aromatic hydrocarbons (PAH) are suspect human lung carcinogens and can be metabolically activated to remote quinones, e.g. benzo[*a*]pyrene-1,6-dione (B[*a*]P-1,6-dione) and B[*a*]P-3,6-dione by the action of either P450 monooxygenase or peroxidases and to non-K region *o*-quinones by aldo-keto reductases (AKRs). B[*a*]P-7,8-dione also structurally resembles 4-hydroxyequilenin *o*-quinone. These three classes of quinones can redox cycle, generate reactive oxygen species (ROS) and produce the mutagenic lesion 8-oxo-dGuo, and may contribute to PAH- and estrogen-induced carcinogenesis. We compared the ability of a complete panel of human recombinant AKRs to catalyze reduction of PAH *o*-quinones in the phenanthrene, chrysene, pyrene and anthracene series. The specific activities for NADPH-dependent quinone reduction were often 100-1,000 times greater than the ability of the same AKR isoform to oxidize the cognate PAH-*trans*-dihydrodiol. However, the AKR with the highest quinone reductase activity for a particular PAH *o*-quinone was not always identical to the AKR isoform with the highest dihydrodiol dehydrogenase activity for the respective PAH-*trans*-dihydrodiol. Discrete AKRs also catalyzed the reduction of B[*a*]P-1,6-dione, B[*a*]P-3,6-dione and 4-hydroxyequilenin *o*-quinone. Concurrent measurements of oxygen consumption, superoxide anion and hydrogen peroxide formation established that ROS were produced as a result of the redox-cycling. When compared with human recombinant NAD(P)H: quinone oxidoreductase (NQO1) and carbonyl reductases (CBR1 and CBR3), NQO1 was a superior catalyst of these reactions followed by AKRs and lastly CBR1 and CBR3. In A549 cells two-electron reduction of PAH *o*-quinones causes intracellular ROS formation. ROS formation was unaffected by the addition of dicumarol suggesting that NQO1 is not responsible for the two-electron reduction observed and does not offer protection against ROS formation from PAH *o*-quinones.

[⊥]To whom correspondence should be addressed: Center for Excellence in Environmental Toxicology, Perelman School of Medicine University of Pennsylvania, 130C John Morgan Building, 3620 Hamilton Walk, Philadelphia, Pennsylvania 19104-6084, USA. Tel: 215-898-9445. Fax: 215-573-7188. penning@upenn.edu.

Keywords

o-quinones; redox-cycling; reactive oxygen species; chemical carcinogenesis; hormonal carcinogenesis

Introduction

[1] PAH are ubiquitous environmental pollutants and suspect human lung carcinogens.[1,2] Two routes of PAH metabolic activation yield dicarbonyls. In the first pathway PAH, e.g. benzo[*a*]pyrene, is activated by either P450 monooxygenases or by peroxidases to yield a radical cation at C6 that gives rise to B[*a*]P-1,6-dione, B[*a*]P-3,6-dione and B[*a*]P-6,12-dione[3] (these metabolites contain carbonyl groups on two different rings and are referred to as remote quinones), Figure 1. The second route involves the NAD(P)$^+$-dependent oxidation of intermediate non-K-region PAH *trans*-dihydrodiols (proximate carcinogens), to yield highly electrophilic and redox active PAH *o*-quinones catalyzed by the dihydrodiol dehydrogenase activity of human aldo-keto reductase (AKR) isoforms (in these metabolites the *trans*-dihydrodiol is present on a terminal benzo-ring). The AKR isoforms responsible for this reaction are AKR1A1 (aldehyde reductase), AKR1C1 (3α(20α)-hydroxysteroid dehydrogenase); AKR1C2 (type 3 3α-hydroxysteroid dehydrogenase); AKR1C3 (type 5 17β-hydroxysteroid dehydrogenase) and AKR1C4 (type 1 3α-hydroxysteroid dehydrogenase).[4–6] The non-K region PAH *o*-quinones formed contain the dicarbonyl on the terminal benzo-ring as shown for B[*a*]P-7,8-dione, Figure 1. Both the remote quinones and the non-K region *o*-quinones can enter into futile redox-cycles, generating reactive oxygen species (ROS) which can lead to DNA strand scission and the formation of the highly mutagenic lesion 8-oxo-2'-deoxyguanosine (8-oxo-dGuo) that may contribute to the carcinogenic process.[7–10]

Recently, intact human lung adenocarcinoma (A549) cells in which AKR isoforms are highly and constitutively expressed were shown to convert B[*a*]P-7,8-dihydrodiol (a *trans*-dihydrodiol) to the corresponding B[*a*]P-7,8-dione, generating intracellular ROS and increasing 8-oxo-dGuo in cellular DNA.[11] Exacerbation of this oxidative stress was observed in the presence of a catechol-*O*-methyl transferase (COMT) inhibitor, suggesting that enzymes that remove the catechol from the redox-cycle are protective against this insult.[11] Similarly, when B[*a*]P-7,8-dione was given to human bronchoalveolar cells (H358) the amount of 8-oxo-dGuo formed in cellular DNA was exacerbated by a COMT inhibitor.[12] The effect of the COMT inhibitor in both cell lines strongly implicates two-electron reduction of the quinone to the catechol as contributing to the ensuing oxidative stress and DNA damage. Importantly, oxidative stress from B[*a*]P-7,8-dione occurs in the presence

[1]Abbreviations: AKRs, aldo-keto reductases, AMPSO, N-(1,1-dimethyl-2-hydroxyethyl)-3-amino-2-hydroxypropanesulfonic acid, androsterone, 3α-hydroxy-5α-androstan-17-one; BA-3,4-dione, benz[*a*]anthracene-3,4-dione; B[*a*]P, benzo[*a*]pyrene; B[*a*]P-7,8-dihydrodiol, (+/−)-*trans*-7,8-dihydroxy-7,8-dihydro-benzo[*a*]pyrene; B[*a*]P-1,6-dione, benzo[*a*]pyrene-1,6-dione; B[*a*]P-3,6-dione, benzo[*a*]pyrene-3,6-dione; B[*a*]P-4,5-dione, benzo[*a*]pyrene-4,5-dione; B[*a*]P-7,8-dione, benzo[*a*]pyrene-7,8-dione; B[*c*]Ph, benzo[*c*]phenanthrene; B[*c*]Ph-3,4-dihydrodiol, (+/−)-*trans*-3,4-dihydroxy-3,4-dihydrobenzo[*c*]phenanthrene; B[*c*]Ph-3,4-dione, benzo[*c*]phenanthrene-3,4-dione; benzo[*g*]chrysene; B[*g*]C, B[*g*]C-11,12-dihydrodiol, (+/−)-*trans*-11,12-dihydroxy-11,12-dihydrobenzo[*g*]chrysene; B[*g*]C-11,12-dione, benzo[*g*]chrysene-11,12-dione; BSA, bovine serum albumin; CBR, carbonyl reductase; C-1,2-dione, chrysene-1,2-dione; C-3,4-dione, chrysene-3,4-dione; COMT, catechol-*O*-methyl transferase; cyt *c*, cytochrome *c*; DB[*a*,*c*]Ph-3,4-dione, dibenzo[*a*,*c*]phenanthrene-3,4-dione; DB[*a*,*l*]P-11,12-dione, dibenzo[*a*,*l*]pyrene-11,12-dione; DCFH-DA, 2',7'-dichlorofluorescein diacetate, DCPIP, dichlorophenolindophenol; DMBA-3,4-dione, dimethylbenz[*a*]anthracene-3,4-dione; dicumarol, 3,3'-methylene-bis(4-hydroxycoumarin); EH, epoxide hydrolase; HBSS, Hanks-Balanced Salt Solution; IPTG, isopropyl ß-D-1-thiogalactopyranoside; 4-OHEN, 4-hydroxyequilenin; 4-OHEN-*o*-quinone, 4-hydroxyequilenin-*o*-quinone; MOPS, 3-(*N*-morpholino)-propanesulfonic acid; LC-MS, liquid chromatography-mass spectrometry; MC-1,2-dione, 5-methylchrysene-1,2-dione; LOD = limit of detection; NQO1, NAD(P)H : quinone oxidoreductase 1; 8-oxo-dGuo, 8-oxo-2'-deoxyguanosine; NP-1,2-dione, naphthalene-1,2-quinone; PAH, polycyclic aromatic hydrocarbon; Ph-9,10-dione, 9,10-phenanthrenequinone; QR, quinone reduction; ROS, reactive oxygen species; SOD, superoxide dismutase.

and absence of the COMT inhibitor suggesting that redox-cycling of the quinone overrides mechanisms that may conjugate and detoxify the intermediate catechol. The human enzymes responsible for the two electron reduction of remote PAH quinones and non-K region quinones to yield the corresponding hydroquinones that in turn contribute to this redox-cycle have not yet been assigned.

Several candidate enzymes exist that could catalyze the two electron reduction of these PAH quinones, including NAD(P)(H) : quinone oxidoreductase (NQO1), carbonyl reductases (CBR1 and CBR3), and AKRs themselves. NQO1 was previously examined as a catalyst of non-K region PAH *o*-quinone reduction using hepatoma cell lysates (H4IIe and HepG2). While dichorophenol-indophenol (DCPIP) reduction could be easily detected in these cell lysates and inhibited by dicumarol no such reduction of the PAH *o*-quinones was observed.[13] Similar results were obtained with rat liver cytosol and this led to the conclusion that two electron reduction of these PAH *o*-quinones was predominately non-enzymatic.[14] Studies on purified human CBR1 characterized PAH *o*-quinone reductase activity with this enzyme.[15] However, only K-region PAH *o*-quinones (which are not proximate carcinogens) were redox-cycled (in these metabolites the dicarbonyl is located on a central benzo-ring). Human placental CBR1 (15-hydroxyprostaglandin dehydrogenase/prostaglandin 9-keto reductase) was reported to catalyze the reduction of PAH *o*-quinones but only the non-K-region *o*-quinone B[*a*]P-7,8-dione was examined.[16,17]

Interestingly, 9,10-phenanthrenequinone (Ph-9,10-dione) which is used as a universal substrate for AKRs can yield the highest catalytic efficiencies for these enzymes.[18-21] However, the major source of quinone reductase that will catalyze the reduction of non-K region PAH *o*-quinones produced by the AKR pathway of PAH activation is not known with certainty. Importantly, these *o*-quinones are structurally related to the *o*-quinones that arise from the catechol estrogens.[22-24] Given the potential role that PAH and estrogen *o*-quinones can play in genotoxic mechanisms of chemical and hormonal carcinogenesis, identification of the quinone reductases that could amplify ROS becomes critically important.

We examined the ability of ten human recombinant AKRs to reduce the remote quinones B[*a*]P-1,6- and 3,6-diones, the non-K region *o*-quinones of PAH in the phenanthrene, chrysene, pyrene and anthracene series, as well as 4-hydroxyequilenin-*o*-quinone (4-OHEN-*o*-quinone), Figure 2. We demonstrate that while AKRs are required for the formation of PAH *o*-quinones in the first place, their proficiency to catalyze PAH *o*-quinone redox-cycling far exceeds their ability to oxidize PAH *trans*-dihydrodiols. We we find that NQO1 is by far the most efficient enzyme for PAH *o*-quinone reduction, followed by AKRs whereas CBR1 and CBR3 play a minimal role. Using human A549 cells two electron reduction of PAH *o*-quinones occurs but dicumarol is without effect suggesting that NQO1 does not participate in this event.

Materials and Methods

Caution

PAHs are potentially hazardous chemicals and should be handled with care in accordance with the NIH Guidelines for Use of Chemical Carcinogens.

Chemicals and Materials

B[*c*]Ph-3,4-dihydrodiol and B[*c*]Ph-3,4-dione were kindly provided by Dr. Mahesh K. Lakshman (The City College and the City University of New York, New York, NY). DB[*a,l*]P-11,12-dione ($\varepsilon_{298.5}$=9,304 $M^{-1}cm^{-1}$ and ε_{360}= 9,211 $M^{-1}cm^{-1}$ in ethanol), B[*g*]C-11,12-dione (ε_{262} = 48,553 M^{-1} cm^{-1} in ethanol), DB[*a,c*]Ph-3,4-dione (ε_{260}= 2749 $M^{-1}cm^{-1}$ in ethanol), C-1,2-dione, C-3,4-dione (ε_{261}=12,721 $M^{-1}cm^{-1}$ and $\varepsilon_{459.5}$= 14,011

$M^{-1}cm^{-1}$ in ethanol), B[*a*]P-1,6-dione, B[*a*]P-3,6-dione, B[*a*]P-7,8-dione, BA-3,4-dione, and 7,12-DMBA-3,4-dione and NP-1,2-dione were synthesized according to published methods. [25,26] MC-1,2-dione was kindly provided by Dr. Shantu Amin (The Pennsylvania State University, Hershey, PA). B[*a*]P-7,8-dihydrodiol, B[*a*]P-4,5-dione, were obtained from the NCI Chemical Carcinogen Standard Reference Repository (Kansas City, MO). Ph-9,10-dione was obtained from Sigma-Aldrich Chemical Co. (St. Louis, MO). Quinones and *trans*-dihydrodiols were analyzed by LC-MS for identity and purity prior to use. The auto-oxidation of 4-OHEN to 4-OHEN-*o*-quinone was monitored by measuring the appearance of the *o*-quinone chromophore (λ_{max}=392 nm) in 10 mM potassium phosphate buffer, pH 7.0, at 37 ºC in air. At 37 ºC, the half life of this quinone was about 1.5 h.[23]

Restriction enzymes were purchased from New England Biolabs (Beverly, MA). NAD^+, $NADP^+$, NADH, and NADPH were obtained from Boehringer Manheim Biochemicals (Indianapolis, IN). *DL*-glyceraldehyde, 3,3'-methylene-bis(4-hydroxycoumarin) (dicumarol), superoxide dismutase (SOD; 4,980 units/mg from bovine erythrocytes), horseradish peroxidase (type II: 200 purpurogallin units/mg), cytochrome *c* (cyt *c*), hypoxanthine, xanthine oxidase (grade I from buttermilk; 17.9 units/mL), catalase (17,600 units/mg from bovine liver), tetramethylbenzidine, AMPSO, and Chromasolv® and DMSO were procured from Sigma-Aldrich Chemical Co. (St. Louis, MO). MOPS was purchased from Fisher Chemicals (Fairlawn, NJ). 1-Acenaphthenol, 2-carboxybenzaldehyde, 4-nitrobenzaldehyde, potassium phosphate and sodium phosphate were purchased from Fisher Chemicals (Fairlawn, NJ). Androsterone was purchased from Steraloids (Wilton, NH). All other chemicals were of the highest grade available, and all solvents for LC-MS were of HPLC grade.

Homogenous human recombinant NQO1 was a kind gift from Dr. David Ross (University of Colorado, Denver, CO). The specific activity was 800 μmol DCPIP reduced/min/mg at 25 ºC. Homogenous human recombinant CBR1 and CBR3 had specific activities of 5,300 μmol/min/mg and 250 μmol/min/mg at 25 ºC, respectively, using Ph-9,10-dione as substrate. CBR1 and CBR3 were purified to homogeneity as previously reported.[27]

Recombinant AKR Enzymes

Homogeneous recombinant AKR1C9 (rat liver 3α-hydroxysteroid/dihydrodiol dehydrogenase) was purified as described.[28,29] The specific activity was 1.6 μmoles androsterone oxidized/min/mg under standard assay conditions.[28] Homogenous recombinant AKR1A1 (aldehyde reductase) was purified as described.5 The specific activity of the enzyme was 6 μmol *p*-nitrobenzaldehyde reduced/min/mg at 25 ºC under standard assay conditions[5]. A pET-23d-AKR1B1 vector was a generous gift from Dr. Mark Petrash (Washington University in St. Louis, St. Louis, MO). AKR1B1 (aldose reductase) was expressed in *E. coli* cells and purified as described.[30] The specific activity was 1.23 μmol *DL*-glyceraldehyde reduced /min/mg at 25 ºC under standard assay conditions.[30] Homogenous recombinant AKR1B10 (small intestine like aldose reductase) was purified as described.[30] The specific activity of the enzyme was 2.1 μmol *DL*-glyceraldehyde reduced/ min/mg at 25 ºC under standard assay conditions.[30] Wild type homogenous recombinant AKR1C1-4 were purified as described.[4] The specific activities were obtained by measuring the NAD^+ dependent oxidation of 1-acenaphthenol and were 2.1 μmol/min/mg (AKR1C1), 2.5 μmol/min/mg (AKR1C2) and 1.8 μmol/min/mg (1C3). For AKR1C4 the specific activity was 0.21 μmol/min/mg for the NAD^+ dependent oxidation of androsterone. All assays were performed at 25 ºC under standard assay conditions.[4,31] Homogenous recombinant AKR1D1 (steroid 5β-reductase) was purified as described.[32] The specific activity was 80 nmoles testosterone reduced/min/mg at 25 ºC under standard assay conditions.[32] Homogenous recombinant AKR7A2 (aflatoxin dialdehyde reductase) was purified as described without its predicted N-terminal extension[18,33] using a pET15b-AKR7A2 vector kindly provided by Dr.

John D. Hayes (University of Dundee). The specific activity of the enzyme was 3.61 μmol 2-carboxybenzaldehyde reduced/min/mg at 25 ºC.

Expression and Purification of Recombinant AKR7A3

AKR7A3 (aflatoxin dialdehyde reductase) was cloned using a ligation-independent cloning strategy. Briefly, the pCMV-SPORT6 vector containing the full-length open reading frame for AKR7A3 (ATCC, Manassas, VA) was linearized with *EcoRI*. AKR7A3 was amplified using the following, forward primer: 5'-dGAC GAC GAC AAG ATG TCC CGG CAG CTG TC-3', and reverse primer: 5'-d GAG GAG AAG CCC GGT TAG CGG AAG TAG TTG GGA CA-3'. The PCR product was treated with T4 DNA polymerase in the presence of dATP to generate complementary overhangs to the pET-46 Ek/LIC vector (Novagen). The annealed pET-46 vector and AKR7A3 insert were transformed into competent *E. coli* cells for recombinant expression as a His_6-fusion protein. Expression of AKR7A3 was induced in *E. coli* with 1 mM IPTG for 3 h. The bacterial pellet was lysed by sonication and applied to a nickel-charged Sepharose column (Amersham Biosciences). Protein was eluted with a linear gradient of 60 to 500 mM imidazole and then dialyzed to remove imidazole. Purity was assessed at each step by SDS-PAGE electrophoresis and by measuring the specific activity of *p*-nitrobenzaldehyde reduction. The final specific activity was 1.03 μmol *p*-nitrobenzaldehyde reduced/min/mg in assays containing 0.2 mM NADPH and 1 mM *p*-nitrobenzaldehyde in 100 mM sodium phosphate buffer, pH 7.0, at 25 °C.

Spectrophotometric Measurement of Enzymatic Quinone Reduction

Non-enzymatic rates of quinone reduction were monitored spectrophotometrically using 10 μM quinone and 180 μM NADPH in 10 mM potassium phosphate buffer, pH 7.0, in the presence of 8% (v/v) DMSO at 37 °C Initial velocities for quinone reduction catalyzed by AKRs were obtained under identical conditions following the addition of a recombinant AKR. Initial velocity measurements were corrected for the non-enzymatic rate of quinone reduction and for the inhibition of each AKR by 8% (v/v) DMSO observed under the standard assay conditions described above. Initial velocity measurements are reported as nmoles/min/mg. At least six replicate measurements were performed with each substrate.

NQO1 was titered by measuring the reduction of 40 μM DCPIP at 600 nm in the presence of 200 μM NADH in 25 mM Tris-HCl, pH 7.4 containing 0.7 mg/ml BSA at 25 °C. NQO1 dilution buffer consisted of 25 mM Tris-HCl (pH 7.4), 250 mM sucrose and 5 μM FAD. Initial velocities for the reduction of quinones catalyzed by NQO1 were obtained using 5 μM quinone and 180 μM NADPH in 10 mM potassium phosphate buffer (pH 7.0) in the presence of 8% (v/v) DMSO 37 ºC. Initial velocities were corrected for non-enzymatic rates and for the inhibition of NQO1 by 8% (v/v) DMSO observed under standard assay conditions. Reactions were replicated six-times.

Initial velocities for the reduction of quinones catalyzed by CBR1 or CBR3 were obtained using 10 μM quinone and 180 μM NADPH in 10 mM potassium phosphate buffer (pH 7.0) in the presence of 10% (v/v) DMSO 37 ºC. Reactions were performed as described above and the reactions were replicated six times.

Oxygen Uptake During Enzymatic Quinone Reduction

The consumption of molecular oxygen was measured in 600 μL reaction chambers containing 10 μM quinone and 60 μM NADPH in 10 mM potassium phosphate buffer (pH 7.0) in the presence of 8% (v/v) DMSO. Reactions were initiated by the addition of 1-5 μg AKR. The output from the microelectrode was connected through an amplifier (Instech, Plymouth Meeting, PA) which allowed the simultaneous display of oxygen concentration and rate of oxygen uptake. Oxidation was monitored over 30 min and data points were taken

every 6 s. Reactions were preformed in duplicate. All oxygen uptake measurements were performed at 37 ºC assuming that the oxygen concentration is 0.117 μmol/600 μL at 760 mm Hg.

Detection of H_2O_2 Production During Enzymatic Quinone Reduction

To detect the formation of H_2O_2 a discontinuous assay was performed. Aliquots (200 μL) were removed from 2 mL reactions (containing 10 μM quinone and 60 μM NADPH in 10 mM potassium phosphate buffer, pH 7.0, in the presence of 8% (v/v) DMSO) over time and were added to 295 μL of solutions containing 338 mM potassium phosphate buffer, pH 6.0 and 338 μM 3,3',5,5'-tetramethylbenzidine. Hydrogen peroxide formation was detected following the addition of 5 μL of 2 mg/mL horseradish peroxidase to the reaction and by measuring the absorbance within 10 s at ε_{650}=30,680 M^{-1} cm^{-1} due to instability of the chromophore. Hydrogen peroxide produced was calculated from a standard curve containing 0 – 40 nmol H_2O_2 where the limit of detection in the assay was 1.0 nmole of hydrogen peroxide. All reactions were performed in duplicate.

Superoxide Anion Radical Production During Enzymatic Quinone Reduction

The NADPH-dependent quinone reductase activity of respective enzymes was linked to the reduction of cyt *c* that was followed at 550 nm. The rate of cyt *c* reduction that was inhibited by superoxide dismutase was taken as a measure of superoxide anion formation. Complete reactions contained: 10 μM quinone and 60 μM NADPH plus 1–5 μg AKR in 10 mM potassium phosphate buffer (pH 7.0) in the presence of 8% (v/v) DMSO plus 60 μM cyt *c* with or without SOD (2000 units/mL). No change in absorbance at 550 nm was detected in the reactions that were devoid of either NADPH, AKR or cyt *c*. Before each reaction was conducted, the ability of superoxide dismutase to completely block the reduction of cyt *c* observed in the presence of 200 μM hypoxanthine plus xanthine oxidase (25 milliunits/mL) was established.

Mammalian Cell Culture

A549 human lung adenocarcinoma cells were obtained from the American Type Culture Collection (ATCC No. CCL-185) and grown as recommended. The cells were treated with B[*a*]P-7.8-dione as follows. 90 ~ 100 % confluent cells were washed with HBSS buffer containing Mg^{2+} and Ca^{2+} and were treated with the same HBSS buffer containing 0 - 20 μM B[*a*]P-7.8-dione, plus 2% (v/v) DMSO as co-solvent.

Detection of Intracellular Reactive Oxygen Species (ROS) Produced by B[*a*]P-7,8-dione

Formation of intracellular ROS in B[*a*]P-7,8-dione-treated A549 cells in the absence or presence of dicumarol was measured using 2',7'-dichlorodihydrofluorescein diacetate (DCFH-DA) dye. A 33.4 mM stock solution of DCFH-DA was freshly prepared in 100 % ethanol purged with N_2. A549 cells (4 x 10^5 cells) in 6 well plates at 50 ~ 60 % confluency were washed 3 times for 5 min with HBSS buffer containing Mg^{2+} and Ca^{2+}. The cells were loaded with 5 mL of 11 μM DCFH-DA in HBSS buffer for 1 h. Excess dye was removed and cells were pretreated with HBSS containing either 20 μM of dicumarol for 0.5 h or with 20 μM dicumarol plus 1 mM desferal and 250 μM α-tocopherol (as antioxidants) for 0.5 h. At the end of the incubation, cells were treated with HBSS containing 5 and 10 μM of B[*a*]P-7,8-dione plus 2% (v/v) DMSO as cosolvent for 6 h. Cells were visualized at 200 x magnification with an epifluorescence microscope (Olympus IX70, Olympus optical co, Japan) (excitation and emission wavelength 495 and 525 nm, respectively). A Clear fluorescent image was obtained when the optical field settings were Low = 491, Hi = 1017, the gamma function = 1.35 and the optimal exposure time was adjusted to 1500 ms. Formation of intracellular ROS was also measured by a fluorescence activated cell sorter

(FACS-calibur, Becton-Dickinson, San Jose, CA) equipped with an argon laser yielding a 488 nm primary emission line. Following treatment cells were harvested using Trypsin-EDTA. A two-parameter dot plot of the side light scatter (SSC) and forward light scatter (FSC) was first analyzed. Then, green fluorescence (FL1-H) was collected in a log scale fashion. The DCF fluorescence of 100,000 cells was measured for control and B[*a*]P-7,8-dione-treated samples. The mean fluorescence intensity (MFI) was analyzed by the FlowJo (Tree Star, Ashland, OR) software program.

Results

Reduction of Non-K region PAH *o*-Quinones by Rat AKR1C9

Rat AKR1C9 catalyzes the $NAD(P)^+$ dependent oxidation of (±)-B[*a*]P-7,8-*trans*-dihydrodiol at initial velocities of 4-6 nmoles/min/mg.[34,35] We also reported that B[*a*]P-7,8-dione was not reduced by a rat liver S9 fraction or by H4IIe or HepG2 cell lysates under conditions in which the NQO1 substrate DCPIP was reduced.[13,14] Unexpectedly, when B[*a*]P-7,8-dione was incubated with NADPH in the presence of homogeneous recombinant AKR1C9 a staggering rate of 4,750 nmoles quinone reduced/min/mg was observed that was enzyme dependent. This prompted us to examine the structural series of PAH *o*-quinones as substrates for AKR1C9 (Table 1). AKR1C9 was found to be a robust catalyst of PAH *o*-quinone reduction in the naphthalene, phenanthrene, chrysene and pyrene series. Specific activities ranged from 0.4 – 5.6 μmoles/min/mg. Interestingly, the remote quinones B[*a*]P-1,6-dione and B[*a*]P-3,6-dione were not substrates for AKR1C9 and 4-hydroxyequilenin-*o*-quinone was a relatively poor substrate for this enzyme.

Reduction of B[*a*]P-7,8-dione by Human AKRs

The ability of human recombinant AKR1A1, AKR1B1 (aldose reductase), AKR1B10 (retinal reductase), AKR1C1-1C4, AKR1D1 (steroid 5β-reductase), AKR7A2, and AKR7A3 (aflatoxin aldehyde reductases) to catalyze the reduction of B[*a*]P-7,8-dione was next examined (see Table 2). Of the AKRs tested, AKR7A2 had the highest rate of reduction with B[*a*]P-7,8-dione and catalyzed a large increase in activity over the rate of non-enzymatic reduction (see, Figure 3A and 4B for representative data). All of the NADPH was consumed in the reduction reactions, revealing the occurrence of a redox-cycling process (i.e., 10 μM quinone consumed 180 μM NADPH). Complete consumption of NADPH was also observed during the reduction of B[*a*]P-7,8-dione catalyzed by AKRs 1A1, 1B1, 1B10, 1C1, 1C2, 1C3, 1C4, and 7A3. By contrast, AKR1D1 failed to catalyze the reduction of any PAH quinone, including B[*a*]P-7,8-dione (Figure 3B). This is consistent with its role in reducing double bonds rather than carbonyl groups.[36,37]

We also compared the ability of the recombinant AKRs to reduce B[*a*]P-7,8-dione with their ability to oxidize (+) or (−) B[*a*]P-7,8-dihydrodiol, Table 2. Specific activity measurements for the dihydrodiol dehydrogenase reaction ranged from 0.13 – 16 nmoles/min/mg, by contrast specific activity measurements for the reduction of B[*a*]P-7,8-dione ranged from 64-1300 nmoles/min/mg. Thus AKRs are superior quinone reductases to dihydrodiol dehydrogenases. Interestingly, AKR7A2 and AKR7A3 do not catalyze the oxidation of PAH *trans*-dihydrodiols yet they gave the highest specific activities for B[*a*]P-7,8-dione reduction. In these and subsequent studies it was not possible to accurately determine k_{cat} and K_m because of the limited solubility of the quinone and thus measurements are reported as specific activities at a constant substrate concentration.

Reduction of other Non-K-Region PAH *o*-Quinones by Human AKRs

We next examined the quinone reductase activity of our panel of human recombinant AKRs using quinones from different structural classes of PAH, Figure 2. Because all the reactions

were performed under identical reaction conditions the specific activities could be directly compared in the form of a heat-map, Table 3. As predicted Ph-9,10-dione was among the best substrates for each of the human AKRs. However, differences were observed in the quinone specificity for each of the AKRs.

For AKR1A1, B[*a*] P-7, 8-dione was the best substrate but neither B[*a*] P-4, 5-dione, BA-3,4-Dione, C-1, 2-dione or C-3, 4-dione were substrates for the enzyme. For AKR1B1, the *fjord*-region PAH *o*-quinones B[*g*]C-11,12-dione and DB[*a,l*]P-11,12-dione were preferred as substrates. The highly related AKR1B10 preferred B[*g*]C-11,12-dione as a substrate over DB[*a,l*]P-11,12-dione which was poorly used. AKR1C1 showed a distinct substrate preference as follows: DB[*a,l*]P-11,12-dione > B[*a*]P-4,5-dione > B[*g*]C-11,12-dione. The preference of AKR1C2 was: B[*a*]P-4,5-dione > DB[*a,l*]P-11,12-dione > B[*a*]P-7,8-dione > B[*g*]C-11,12-dione. By contrast AKR1C3 reduced DB[*a,l*]P-11,12-dione at specific activities of only 5% of 10% of that seen with either AKR1C1 or AKR1C2, respectively. AKR1C4 showed relatively poor quinone reductase activity among the range of substrates tested. AKR7A2 showed a distinct preference for B[*a*]P-7,8-dione, B[*a*]P-4,5-dione and DB[*a,l*]P-11,12-dione and was the only enzyme that could reduce the *o*-quinones in the benz[*a*]anthracene series. AKR7A3 like AKR7A2 preferred B[*a*]P-7,8-dione and B[*a*]P-4,5-dione but could not reduce DB[*a,l*]P-11,12-dione well. Of the AKRs tested AKR7A2 was the superior enzyme for the reduction of the majority of the PAH *o*-quinones tested.

Reduction of Remote PAH-quinones by Human AKRs

Only AKR1C1 and AKR1C3 gave specific activites for the reduction of the remote quinones B[*a*]P-1,6-dione and B[*a*]P-3,6-dione that were similar to the activities they displayed with B[*a*]P-7,8-dione. AKR1A1, 1B10, 1C2 and 7A2 displayed at least 10-50-fold lower specific activities with B[*a*]P-1,6-dione and B[*a*]P-3,6-dione than with B[*a*]P-7,8-dione. These remote quinones were not substrates for AKR1B1 and 1C4, while AKR7A3 catalyzed a modest reduction of B[*a*]P-1,6-dione. In general remote B[*a*]P-quinones were poor substrates for AKRs.

Reduction of 4-OHEN *o*-Quinone by Human AKRs

The ability of human AKRs to reduce 4-OHEN *o*-quinone, which shares structural similarities with non-K region PAH *o*-quinones was examined. Specific activites for the reduction of 4-OHEN-*o*-quinone catalyzed by human AKRs are shown in Table 4. AKR1B1, 1C1, 1C2, 1C3 and 7A2 all reduce 4-OHEN *o*-quinone. AKR7A2 demonstrated the highest specific activity, followed by AKR1B1. AKR1C1 and AKR1C2 displayed the lowest specific activity with this substrate.

Generation of Reactive Oxygen Species During the Redox-cycling of Quinones by AKRs

The ability of each AKR reaction containing 10 μM quinone and 180 μM NADPH to deplete all the cofactor present suggests that redox-cycling was occurring. To confirm that ROS were produced we monitored the consumption of molecular oxygen as well as the appearance of superoxide anion and hydrogen peroxide in reactions containing AKR isoforms and compounds representative of each of the major classes of diones tested, i.e. B[*a*]P-3,6-dione (B[*a*]P-remote quinone), B[*a*]P-7,8-dione (non-K region PAH *o*-quinone), and 4-OHEN-*o*-quinone (catechol estrogen quinone), Figures 4A-L. During the reduction of B[*a*]P-3,6-dione catalyzed by AKR1C3 or the reduction of B[*a*]P-7,8-dione and 4-OHEN-*o*-quinone catalyzed by AKR7A2, consumption of molecular oxygen and the concomitant production of superoxide anion and hydrogen peroxide was observed. In each case the amounts of NADPH consumed and H_2O_2 formed were stoichiometric, consistent with equations 1–3:

$$Q+NADPH+H^+ \rightarrow QH_2+NADP^+ \quad \text{Eqn. 1}$$

$$QH_2+O_2 \rightarrow Q+H_2O_2 \quad \text{Eqn. 2}$$

$$NADPH+H^++O_2 \rightarrow NADP^++H_2O_2 \quad \text{Eqn. 3}$$

Where Q = quinone and QH_2 = hydroquinone.

Comparison of the Quinone Reductase Activity of NQO1, AKRs and CBR1 and CBR2

We next compared AKR7A2 which is the AKR with the highest quinone reductase specific activity with NQO1 and CBR1 or CBR3 to determine which of these enzymes was the superior catalyst for the reduction of the various quinones tested, Table 5. The following features were apparent. First, NQO1 was the preferred enzyme for quinone reduction followed by AKR7A2 followed by CBR1 and CBR3. Second, NQO1 was the only enzyme that showed robust activity for the reduction of the remote quinones: B[*a*]P-1,6-dione, B[*a*]P-3,6-dione. Third, there were some notable exceptions to these rules. B[*a*]P-7,8-dione and DB[*a,l*]P-11,12-dione were reduced equally well by NQO1 and AKR7A2. Fourth, CBR1 preferred the reduction of K-region *o*-quinones, e.g. Ph-9,10-dione and B[*a*]P-4,5-dione and CBR3 was a relatively poor quinone reductase using any PAH *o*-quinone. Fifth, 4-OHEN *o*-quinone was reduced with a high specific activity by NQO1 with only a modest contribution from AKR7A2.

NQO1 is Not the Dominant QR responsible for the B[*a*]P-7,8-dione Reduction in A549 Cells

We previously showed that B[*a*]P-7,8-dione can cause intracellular ROS formation in A549 cells using DCFH-DA fluorescence.[11] We also found that A549 cells highly express NQO1 based on functional activity as measured by the ability to reduce DCPIP and found that over 90% of this activity can be abolished by the addition of 20 μM dicumarol (data not shown). These cells also contain substantial AKR activity as measured by using their standard substrates (see, Materials and Methods, data not shown). [6] We also showed that the addition of a COMT inhibitor would exacerbate ROS formation from cells treated with either B[*a*]P-7,8-dihydrodiol or B[*a*]P-7,8-dione implying that when the catechol was not conjugated, two electron redox-cycling involving the auotoxidation of the catechol to B[*a*]P-7,8-dione was increased. We reasoned that if NQO1 was responsible for the two electron redox-cycling, dicumarol would eliminate ROS production. We also reasoned that if NQO1 was performing a protective role then dicumarol treatment would exacerbate ROS formation. Neither affect was observed. We find that the increase in DCFH-DA fluorescence seen with dicumarol was entirely attributable to the fluorescence of dicumarol itself. These data suggest that two electron reduction contributes to the ROS generated by PAH *o*-quinones but NQO1 is not involved in this process. Unfortunately, the direct involvement of AKRs in the process is not testable using either pharmacologic or genetic manipulation. A549 cells express a panel of AKRs and no single inhibitor will block their activity; similarly it is not feasible to use a sh-RNA approach to knock down the complete panel of AKR that is expressed.

Discussion

In this study we provide compelling evidence that human AKRs catalyze the two electron reduction of PAH *o*-quinones in the naphthalene, phenanthrene, chrysene, pyrene and benz[*a*] anthracene series. We demonstrate that this activity results in redox-cycling with the concomitant formation of ROS (superoxide anion and hydrogen peroxide). Remarkably, the specific activities for *o*-quinone reduction exceed the rates of PAH *trans*-dihydrodiol oxidation catalyzed by AKRs by several orders of magnitude. Importantly, two of the AKRs most proficient at *o*-quinone reduction, AKR7A2 and AKR7A3, do not oxidize their PAH *trans*-dihydrodiol precursors. This leads to the prediction that human AKR1A1, and AKR1C1-1C4 are the dominant isoforms that oxidize proximate carcinogenic PAH *trans*-dihydrodiols to their corresponding *o*-quinone. However, once formed by these relatively slow enzyme catalyzed reactions there is rapid and profound 2 electron redox cycling of the PAH *o*-quinones and that the AKRs involved can differ from those that were required to form the PAH *o*-quinones in the first place. Although NQO1 can often act as a superior catalyst for PAH *o*-quinone reduction *in vitro,* its physiological role in this process in lung cells is ruled out due to the inability of dicumarol to block two electron reduction of PAH *o*-quinones in A549 human lung adenoacarcinoma cells. Before this study it was widely accepted that NQO1 was the most robust catalyst for the two electron reduction of quinones in cells[38].

Lattice Models of AKR Active Sites

The ten human recombinant AKR enzymes (AKR1A1, 1B1, 1B10, 1C1-1C4, 1D1, 7A2 and 7A3) displayed quite different quinone reductase activities on the panel of substrates tested. These differences were exploited to build lattice structures of how these PAH *o*-quinones may be accommodated at the AKR active sites to account for the observed specificity differences. For example, AKR1A1 will turnover B[*a*]P-7,8-dione and B[*g*]C-11,12-dione but not C-1,2-dione, C-3,4-dione, BA-3,4-dione or B[*a*]P-4,5-dione suggesting that the non-substrates are excluded from the active site. Superimposition of PAH *o*-quinones that are AKR1A1 substrates yields the black lattice structure for included substrates and superimposition of PAH *o*-quinones that are non-substrates for AKR1A1 yields the red lattice structure for excluded substrates, Fig. 6E. For example, B[*a*]P-7,8-dione rings 1-5 are in the bound orientation while B[*a*]P-4,5-dione rings 1'-5' are in the unbound orientation, Fig. 6E. AKR1B1 and AKR1B10 do not turnover DB[*c*]Ph-3,4-dione rings 1-5 but differ in that the former will turnover C-3,4-dione rings 1'-4' giving rise to the lattice models proposed in Fig. 6F - G. AKR1C1 and AKR1C2 display similar substrate specificity for the reduction of PAH *o*-quinones consistent with their greater than 99% sequence identity. Their ability to both reduce DB[*a,l*]P-11,12-dione can be explained by the lattice model in Fig. 6H. AKR1C3 differs from AKR1C1 and AKR1C2 since it reduces DB[*a,l*]P-11,12-dione poorly and can be explained by the lattice model in Fig. 6I. In the AKR1C lattice structures the rings of DB[*a,l*]P-11,12-dione are numbered 1-6. AKR1C4 shows predominately a preference for B[*a*]P-7,8-dione (ring numbering 1-5) and B[*a*]P-4,5-dione (ring numbering 1'-5'), and these findings can be explained by the lattice model proposed for AKR1C4 Fig 6J. However, it is a relatively poor quinone reductase for the range of PAH *o*-quinones tested. AKR7A2 differs from AKR7A3 in that it reduces BA-3,4-dione and DMBA-3,4-dione yielding the lattice structures in Fig 6K and L (where the ring numbering for BA is shown 1-4). In fact AKR7A2 is the only AKR isoform that will reduce PAH *o*-quinones in the benz[*a*]anthracene series.

Evidence for Redox-Cycling Catalyzed by AKRs

The ability of recombinant AKRs to redox-cycle three functional classes of quinone substrates (PAH remote quinones, PAH *o*-quinones, and 4-OHEN-*o*-quinone) is supported

by the complete consumption of greater than stoichiometric amounts of NADPH, the concomitant consumption of molecular oxygen, and formation of superoxide anion and hydrogen peroxide. Raising the issue of whether this event contributes to the inactivation of PAH *o*-quinones or their toxicity. In this respect, the major enzyme implicated in two electron reduction of PAH quinones and prevent quinone mediated toxicity is NQO1.[38,39]

Comparison of the Quinone Reductase Activities of NQO1, AKR, CBR1 or CBR3 and their Roles in Quinone Mediated Toxicity

Comparison of recombinant NQO1, AKR and CBR1 and CBR3, revealed that NQO1 is the preferred NADPH dependent two electron quinone reductase for the substrates tested. The involvement of NQO2 in the two electron redox-cycling of *o*-quinones was not examined since it has a requirement for dihydronicotinamide riboside as a cofactor instead of the major cellular reducing equivalent NADPH. Two *o*-quinones, B[*a*]P-7,8-dione and DB[*a,l*]P-11,12-dione derived from the potent pro-carcinogens B[*a*]P and DB[*a,l*]P-11,12-dione, respectively were better substrates for AKR7A2 than for NQO1.

NQO1 has been implicated as an important enzyme that protects cells from quinone mediated toxicity. In our studies NQO1 was the only enzyme that catalyzed the robust reduction of the remote quinones, e.g. B[*a*]P-1,6-dione and B[*a*]P-3,6-dione. Previously menadione, B[*a*]P-3,6-dione, and Ph-9,10-dione were all shown to be mutagenic in a *Salmonella* tester strain with an S9 bioactivation system where NADPH-P450 oxidoreductase catalyzed one-electron reduction of the quinones to their semiquinone radicals.[39] Addition of dicumarol did not alter the number of revertants, indicating that NQO1-catalyzed two-electron reduction of these quinones did not contribute to mutagenicity. Transfection of NQO1 in COS-1 cells expressing NADPH-P450 reductase and P450 1A1 decreased covalent B[*a*]P, B[*a*]P-3,6-dione, and B[*a*]P-6,12-dione–DNA adducts measured by [^{32}P]-postlabeling and this effect was reversed with dicumarol[40]. Together these data support the concept that NQO1 protects against quinone mediated toxicity. However, it is unclear whether this protective role of NOQ1 is applicable to different structural classes of quinones as well as other quinone reductases that catalyze two electron reduction.

The toxicity of quinone exposure will depend upon respective rates of hydroquinone/catechol conjugation versus the propensity to be re-oxidized in air and redox-cycle. Rates of quinone reduction are also controlled by the availability of NADPH and the K_m values of the candidate enzymes for this cofactor. For NQO1 the K_m values for NAD(P)H are similar at 130 -180 μM.[41] For AKRs the K_d for NADPH can be between 9 – 120 nM and the K_m values are between 0.01 – 2.0 μM.[42,43] Thus at the prevailing cellular NADPH concentrations the AKRs will be completely saturated and may be the more efficient quinone reductases.

In cell based assays the contribution of AKR mediated two electron reduction to PAH *o*-quinone toxicity may be inferred based on several observations. First, ROS production is seen in A459 cells treated with PAH *trans*-dihydrodiols and PAH *o*-quinones.[11] Second, A459 cells contain a high level of constitutive expression of AKR isozymes.[6] Third, 8-oxo-dGuo and DNA strand breaks are elevated in cells treated with *trans*-dihydrodiols and a COMT inhibitor suggesting a catechol/*o*-quinone based redox-cycle is occurring.[11,12] Fourth, these cells contain a high level of NQO1 activity that can be inhibited by dicumarol by over 90% but treatment with dicumarol does not eliminate or exacerbate ROS formation in PAH *o*-quinone exposed cells. This suggests that NQO1 is not involved in the intracellular redox-cycling of the PAH *o*-quinones and does not protect against the deleterious effects of the *o*-quinones in this setting. Fifth, although NQO1 has higher specific activities for PAH *o*-quinone reduction than observed by any individual AKR, most

cells contain a panel of AKR enzymes suggesting that their combined quinone reductase activity may exceed that observed with NQO1. Sixth unlike NQO1, AKRs have nanomolar affinity for NADPH suggesting that they are fully saturated at physiologic cofactor concentrations to conduct redox-cycling of PAH *o*-quinones.[43,44] Interestingly like NQO1, AKR1C1-AKR1C3 and AKR1B10 are all induced by ROS acting through an antioxidant response element[45–49] suggesting that a positive feedback loop exists that could exacerbate ROS formation and contribute to PAH induced oxidative stress. Based on the importance of AKRs in the redox-cycling process it is necessary to consider tissue levels of AKRs as it relates to PAH-exposure.

Tissue Distribution of AKRs and PAH-Toxicity

AKR1A1 displays the highest catalytic efficiency for the oxidation of (–)-B[*a*]P-7,8-*trans*-dihydrodiol.[5] By contrast, AKR1A1 has the lowest quinone reductase activity of all AKR isoforms with each type of quinone examined. RT-PCR revealed that AKR1A1 levels in normal human bronchoalveolor cells are very low.[50,51] These findings suggest that it is unlikely that AKR1A1 plays a major role in ROS generation from PAH *o*-quinones in the lung.

AKR1B1 and 1B10 have a low catalytic efficiency for the oxidation of PAH *trans*-dihydrodiols. Also, these enzymes displayed stereospecificity for the minor isomers of PAH *trans*-dihydrodiol formed metabolically. This implies that these enzymes play a minor role in oxidation of PAH *trans*-dihydrodiols.[30] However, in the reductive direction, AKR1B10 showed wide substrate specificity with PAH *o*-quinones. This isoform had the highest rates of quinone reduction with PAH *o*-quinones in the chrysene series suggesting that AKR1B10 may play an important role in oxidative damage mediated by quinones from this tobacco carcinogen. Because of the high expression of AKR1B10 in non-small cell lung carcinoma and because it is a smoking exposure and response gene.[52–54] AKR1B10 may play a role in human lung carcinogenesis via the redox-cycling of chrysene *o*-quinones.

AKR isoforms 1C1-1C3 all convert PAH *trans*-dihydrodiols to *o*-quinones and are often the most catalytically efficient of all AKR isoforms examined for these reactions.[6] AKR1C1, 1C2, and 1C3 showed increasing rates of quinone reduction in the chrysene series as a result of bay-region substitution either with a methyl group or by the introduction of a benzo-ring to create a *fjord* region. The specific activity of AKR1C3 and AKR1B10 for B[*g*]C-1,2-dione was similar. In A549 cells, AKR1C2 expression levels are approximately 3 times higher than AKR1C1 or AKR1C3 which may suggest that AKR1C isoforms may play large roles in catalyzing oxidative damage from bay-ring substituted *o*-quinones in the lung.[6]

AKR7A2 and AKR7A3 are the only AKR isoforms examined that are unable to oxidize PAH *trans*-dihydrodiols to form PAH *o*-quinones. However, AKR7A2 was the only isoform examined able to reduce BA-3,4-dione and DMBA-3,4-dione. It showed the highest specific activity with small PAH *o*-quinones like NP-1,2-dione and Ph-9,10-dione, the second highest specific activity with *fjord*-region PAH *o*-quinones, and demonstrated equal rates of quinone reduction with K- and non-K region PAH *o*-quinones alike. In general, this isoform was the preferred AKR isoform involved in quinone reduction. Although AKR7A2 is expressed in A549 cells, it is present in smaller amounts than either the AKR1B or AKR1C isoforms.[30]

Reduction of 4-OHEN *o*-Quinone

We and others have drawn parallels between the genotoxic mechanisms mediated by PAH *o*-quinones with those generated by the catechol estrogens and their corresponding quinones, e.g. 4-OHEN-*o*-quinone.[55,56] Because of these similarities, we examined the role of NQO1,

AKRs and CBRs in the redox-cycling of this quinone. We found that NQO1 was able to catalyze the NADPH-dependent reduction of 4-OHEN-*o*-quinone with a specific activity 100 times higher than that observed for AKR7A2 which had the highest activity of any AKR. However, it has been proposed that the high activity observed for 4-estrogen-*o*-quinone with NQO1 is unlikely to contribute to the redox-cycling of this estrogen metabolite since this is only observed when supraphysiologic concentrations of the *o*-quinone are used as substrate.[57]

Summary

The two-electron quinone reductases, which enhance ROS formation by reducing B[*a*]P-remote quinones, non-K region PAH *o*-quinones and 4OHEN-o-quinone to their corresponding hydroquinones were identified. NQO1 and the AKRs were the major enzymes involved in these processes. While AKRs are required for the oxidation of PAH *trans*-dihydrodiols to form PAH *o*-quinones, their ability to significantly enhance the redox-cycling of the *o*-quinones *in vitro* and in lung cells was unexpected. While NQO1 had higher specific activities than AKRs, the K_m for NADPH with NQO1 is two orders of magnitude higher than that seen with AKRs, which limits the protective role of NQO1 in cells. We infer that AKRs play a significant role in PAH *o*-quinone reduction and contribute to their cytotoxicity and mutagenicity.

Acknowledgments

Funding Source This study was supported by NIH Grants PO1-CA92537, P30-ES 013508, RO1-CA39504 and PA-DOH4100038714 (awarded to T.M.P.).

We thank Dr. Rebekka Mindnich for her cloning expertise.

References

1. Hecht SS. Tobacco smoke carcinogens and lung cancer. J Natl Cancer Institute. 1991; 91:1194–1210.
2. World Health Organization. IARC Monographs on the Evaluation of Carcinogenic Risks to Humans. Vol. 92. Lyons, France: 2010. Some non-heterocyclic polycyclic aromatic hydrocarbons and some related exposures.
3. Cavalieri EL, Rogan EG. Central role of radical cations in the metabolic activation of polycyclic aromatic hydrocarbons. Xenobiotica. 1995; 25:677–688. [PubMed: 7483666]
4. Burczynski ME, Harvey RG, Penning TM. Expression and characterization of four recombinant human dihydrodiol dehydrogenase isoforms: Oxidation of *trans*-7,8-dihydroxy-7,8-dihydrobenzo[*a*]pyrene to the activated *o*-quinone metabolite benzo[*a*]pyrene-7,8-dione. Biochemistry. 1988; 37:6781–6790. [PubMed: 9578563]
5. Palackal NT, Burczynski ME, Harvey RG, Penning TM. The ubiquitous aldehyde reductase (AKR1A1) oxidizes proximate carcinogen *trans*-dihydrodiols to *o*-quinones: Potential role in polycyclic aromatic hydrocarbon activation. Biochemistry. 2001; 40:10901–10910. [PubMed: 11535067]
6. Palackal NT, Lee SH, Harvey RG, Blair IA, Penning TM. Activation of polycyclic aromatic hydrocarbon *trans*-dihydrodiol proximate carcinogens by human aldo-keto reductase (AKR1C) enzymes and their functional overexpression in human lung adenocarcinoma (A549) cells. J Biol Chem. 2002; 277:24799–24808. [PubMed: 11978787]
7. Flowers L, Ohnisni ST, Penning TM. DNA strand scission by polycyclic aromatic hydrocarbon *o*-quinones: role of reactive oxygen species. Cu(II)/Cu(I) redox cycling, and *o*-semiquinone anion radicals. Biochemistry. 1997; 36:8640–8648. [PubMed: 9214311]
8. Lorentzeen RJ, Ts' O POP. Benzo[*a*]pyrenedione/benzo [*a*]pyrenediol oxidation-reduction couples and the generation of reactive reduced molecular oxygen. Biochemistry. 1977; 16:1467–1473. [PubMed: 191070]

9. Park JH, Gopishetty S, Szewczuk LM, Troxel AB, Harvey RG, Penning TM. Formation of 8-oxo-7,8-dihydro-2'-deoxyguanosine (8-oxo-dGuo) by PAH *o*-quinones: involvement of reactive oxygen species and copper (II)/copper(I) redox cycling. Chem Res Toxicol. 2005; 18:1026–1037. [PubMed: 15962938]
10. Park JH, Gelhaus S, Vedantam S, Olivia A, Batra A, Blair IA, Field J, Penning TM. The pattern of p53 mutations caused by PAH *o*-quinones is driven by 8-oxo-dGuo formation while the spectrum of mutations is determined by biological selection for dominance. Chem Res Toxicol. 2008; 21:1039–49. [PubMed: 18489080]
11. Park JH, Mangal D, Tacka KA, Quinn AM, Harvey RG, Blair IA, Penning TM. Evidence for the aldo-keto reductase pathway of polycyclic aromatic *trans*-dihydrodiol activation in human lung A549 cells. Proc Natl Acad Sci U S A. 2008; 105:6846–51. [PubMed: 18474869]
12. Mangal D, Vudathala D, Park JH, Lee DH, Penning TM, Blair IA. Analysis of 7,8-dihydro-8-oxo-2'-deoxyguanosine in cellular DNA during oxidative stress. Chem Res Toxicol. 2009; 22:788–97. [PubMed: 19309085]
13. Flowers-Geary L, Bleczinski W, Harvey RG, Penning TM. Cytotoxicity and mutagenicity of polycyclic aromatic hydrocarbon *o*-quinones produced by dihydrodiol dehydrogenase. Chemico-Biol Inter. 1996; 99:55–72.
14. Flowers-Geary L, Harvey RG, Penning TM. Examination of polycyclic aromatic hydrocarbon *o*-quinones produced by dihydrodiol dehydrogenase as substrates for redox-cycling in rat liver. Biochem (Life Sci Adv). 1992; 11:49–58.
15. Wermuth B, Platt KL, Seidel A, Oesch F. Carbonyl reductase provides the enzymatic basis of quinone detoxication in man. Biochem Pharmacol. 1986; 35:1277–82. [PubMed: 3083821]
16. Jarabak J. Polycyclic aromatic hydrocarbon quinone-mediated oxidation reduction cycling catalyzed by a human placental NADPH-linked carbonyl reductase. Arch Biochem Biophys. 1991; 29:334–8. [PubMed: 1659323]
17. Jarabak J. Polycyclic aromatic hydrocarbon quinones may be either substrates for or irreversible inhibitors of the human placental NAD-linked 15-hydroxyprostaglandin dehydrogenase. Arch Biochem Biophys. 1992; 292:239–43. [PubMed: 1309294]
18. Ireland LS, Harrison DJ, Neal GE, Hayes JD. Molecular cloning, expression and catalytic activity of a human AKR7 member of the aldo-keto reductase superfamily: evidence that the major 2-carboxybenzaldehyde reductase from human liver is a homolog of rat aflatoxin B_1-aldehyde reductase. Biochem J. 1988; 332:21–34. [PubMed: 9576847]
19. Matsunaga T, Arakaki M, Kamiya T, Endo S, El-Kabbani O, Hara A. Involvement of an aldo-keto reductase (AKR1C3) in redox-cycling of 9,10-phenanthrenequinone leading to apoptosis in human endothelial cells. Chemico Biol Inter. 2009; 181:52–60.
20. Oppermann U. Carbonyl reductases: the complex relationships of mammalian carbonyl-quinone-reducing enzymes and their role in physiology. Annu Rev Pharmacol Toxicol. 2007; 47:292–322.
21. Penning TM, Mukharji I, Barrows S, Talalay P. Purification and properties of a 3α-hydroxysteroid dehydrogenase of rat liver cytosol and its inhibition by anti-inflammatory drugs. Biochem J. 1984; 222:601–611. [PubMed: 6435601]
22. Chen Y, Shen L, Zhang F, Lau SS, van Breemen RB, Nikolic D, Bolton JL. The equine estrogen metabolite 4-hydroxyequilenin causes DNA single-strand breaks and oxidation of DNA bases *in vitro*. Chem Res Toxicol. 1998; 11:1105–11. [PubMed: 9760286]
23. Shen L, Pisha E, Huang Z, Pezzuto JM, Krol E, Alam Z, van Breemen RB, Bolton JL. Bioreductive activation of catechol estrogen-*ortho*-quinones: aromatization of the B ring in 4-hydroxyequilenin markedly alters quinoid formation and reactivity. Carcinogenesis. 1997; 18:1093–101. [PubMed: 9163701]
24. Zhang F, Swanson SM, van Breemen RB, Liu X, Yang Y, Gu C, Bolton JL. Equine estrogen metabolite 4-hydroxyequilenin induces DNA damage in the rat mammary tissues: formation of single-strand breaks, apurinic sites, stable adducts, and oxidized bases. Chem Res Toxicol. 2001; 14:1654–9. [PubMed: 11743748]
25. Harvey RG, Dai Q, Ran C, Penning TM. Synthesis of the *o*-quinones and other oxidized metabolites of polycyclic aromatic hydrocarbons implicated in carcinogenesis. J Org Chem. 2004; 69:2024–2032. [PubMed: 15058949]

26. Penning TM. Aldo-keto reductases and formation of polycyclic aromatic hydrocarbon *o*-quinones. Methods Enzymol. 2004; 378:31–67. [PubMed: 15038957]
27. El-Hawari Y, Favia AD, Pilka ES, Kisiela M, Oppermann U, Martin HJ, Maser E. Analysis of the substrate-binding site of human carbonyl reductases CBR1 and CBR3 by site-directed mutagenesis. Chemico Biol Inter. 2009; 181:52–60.
28. Pawlowski JE, Penning TM. Overexpression and mutagenesis of the cDNA for rat liver 3α-hydroxysteroid/dihydrodiol dehydrogenase. Role of cysteines and tyrosines in catalysis. J Biol Chem. 1994; 269:13502–10. [PubMed: 8175784]
29. Ratnam K, Ma H, Penning TM. The arginine 276 anchor for NADP(H) dictates fluorescence kinetic transients in 3α-hydroxysteroid dehydrogenase, a representative aldo-keto reductase. Biochemistry. 1999; 38:7856–64. [PubMed: 10387026]
30. Quinn AM, Harvey RG, Penning TM. Oxidation of PAH *trans*-dihydrodiols by human aldo-keto reductase AKR1B10. Chem Res Toxicol. 2009; 21:2207–15. [PubMed: 18788756]
31. Jin Y, Duan L, Lee SH, Kloosterboer HJ, Blair IA, Penning TM. Human cytosolic hydroxysteroid dehydrogenases of the aldo-ketoreductase superfamily catalyze reduction of conjugated steroids: Implications for phase I and phase II steroid hormone metabolism. J Biol Chem. 2009; 284:10013–22. [PubMed: 19218247]
32. Di Costanzo L, Drury JE, Penning TM, Christianson DW. Crystal structure of human liver Δ^4–3-ketosteroid 5β-reductase (AKR1D1) and implications for substrate binding and catalysis. J Biol Chem. 2008; 283:16830–9. [PubMed: 18407998]
33. Kelly VP, Shearratt PJ, Coruch DH, Hayes JD. Novel homodimeric and heterodimeric rat gamma-hydroxybutyrate synthases that associate with the Golgi apparatus define a distinct subclass of aldo keto reductase 7 family proteins. Biochem J. 2002; 366:847–61. [PubMed: 12071861]
34. Flowers-Geary L, Harvey RG, Penning TM. Examination of diols and diol-epoxides of polycyclic aromatic hydrocarbons as substrates for rat liver dihydrodiol dehydrogenase. Chem Res Toxicol. 1992; 5:576–583. [PubMed: 1391625]
35. Smithgall TE, Harvey RG, Penning TM. Regio- and stereospecificity of homogeneous 3α-hydroxysteroid-dihydrodiol dehydrogenase for *trans*-dihydrodiol metabolites of polycyclic aromatic hydrocarbons. J Biol Chem. 1986; 261:6184–6191. [PubMed: 3457793]
36. Chen M, Drury JE, Penning TM. Substrate specificity and inhibitor analyses of human steroid 5β-reductase (AKR1D1). Steroids. 2011; 76:484–90. [PubMed: 21255593]
37. Kondo KH, Kai MH, Setoguchi Y, Eggertsen G, Sjoblom P, Setoguchi T, Okuda KI, Bjorkhem I. Cloning and expression of cDNA of human Δ4–3-oxosteroid-5β-reductase and substrate specificity of the expressed enzyme. Eur J Biochem. 1994; 219:357–363. [PubMed: 7508385]
38. Lind C, Hochstein P, Ernster L. DT-Diaphorase as a quinone reductase: A cellular control device against semiquinone and superoxide radical formation. Arch Biochem Biophys. 1982; 216:178–185. [PubMed: 6285828]
39. Chesis PL, Levin DE, Smith MT, Ernster L, Ames BN. Mutagenicity of quinones: pathways of metabolic activation and detoxification. Proc Natl Acad Sci U S A. 1994; 81:1696–1700. [PubMed: 6584903]
40. Joseph P, Jaiswal AK. NAD(P)H:quinone oxidoreductase1 (DT-diaphorase) specifically prevents the formation of benzo[*a*]pyrene quinone-DNA adducts generated by cytochrome P4501A1 and P450 reductase. Proc Natl Acad Sci USA. 1994; 91:8413–8417. [PubMed: 8078896]
41. Ernster L, Danielson L, Ljunggren M. DT-diaphorase I. Purification from the soluble fraction of rat-liver cytoplasm and properties. Biochim Biophys Acta. 1962; 58:171–188. [PubMed: 13890666]
42. Grimshaw CE, Bohren KM, Lai CJ, Gabbay KH. Human aldose reductase: rate constants for a mechanism including interconversion of ternary complexes by recombinant wild-type enzyme. Biochemistry. 1995; 34:14356–65. [PubMed: 7578039]
43. Jin Y, Penning TM. Multiple steps determine the overall rate of the reduction of 5a-dihydrotestosterone catalyzed by human type 3 3a-hydroxysteroid dehydrogenase: implications for the elimination of androgens. Biochemistry. 2006; 45:13054–63. [PubMed: 17059222]
44. Cooper WC, Jin Y, Penning TM. Elucidation of a complete kinetic mechanism for a mammalian hydroxysteroid dehydrogenase (HSD) and identification of all enzyme forms on the reaction

coordinate: The example of rat liver 3α-HSD (AKR1C9). J Biol Chem. 2007; 282:33484–93. [PubMed: 17848571]

45. Dinkova-Kostova AT, Talalay P. NAD(P)H:quinone acceptor oxidoreductase 1 (NQO1), a multifunctional antioxidant enzyme and exceptionally versatile cytoprotector. Arch Biochem Biophys. 2010; 501:116–123. [PubMed: 20361926]
46. Burczynski ME, Lin HK, Penning TM. Isoform-specific induction of a human aldo-keto reductase by polycyclic aromatic hydrocarbons (PAHs), electrophiles, and oxidative stress: implications for the alternative pathway of PAH activation catalyzed by human dihydrodiol dehydrogenases. Cancer Res. 1999; 59:607–614. [PubMed: 9973208]
47. Lou H, Du S, Ji Q, Stolz A. Induction of AKR1C2 by phase II inducers: identification of a distal consensus antioxidant response element regulated by Nrf2. Mol Pharmacol. 2006; 69:1662–72. [PubMed: 16478829]
48. MacLeod AK, McMahon M, Plummer SM, Higgins LG, Penning TM, Igarashi K, Hayes JD. Characterization of the cancer chemopreventive NRF2-dependent gene battery in human keratinocytes: demonstration that the KEAP1-NRF2 pathway, and not the BACH1-NRF2 pathway, controls cytoprotection against electrophiles as well as redox-cycling compounds. Carcinogenesis. 2009; 30:1571–80. [PubMed: 19608619]
49. Agyeman AS, Chaerkady R, Shaw PG, Davidson NE, Visvanathan K, Pandey A, Kensler TW. Transcriptomic and proteomic profiling of KEAP1 disrupted and sulforaphane-treated human breast epithelial cells reveals common expression profiles. Breast Cancer Res Treat. 2011 May 20. [Epub ahead of print].
50. Jiang H, Vudathala DK, Blair IA, Penning TM. Competing roles of aldo-keto reductase 1A1 and cytochrome P4501B1 in benzo[*a*]pyrene-7,8-diol activation in human bronchoalveolar H358 cells: Role of AKRs in P4501B1 induction. Chem Res Toxicol. 2006; 19:68–78. [PubMed: 16411658]
51. Quinn AM, Penning TM. Comparisons of (+/−)-benzo[a]pyrene-*trans*-7,8-dihydrodiol activation by human cytochrome P450 and aldo-keto reductase enzymes: effect of redox state and expression levels. Chem Res Toxicol. 2008; 21:1086–94. [PubMed: 18402469]
52. Fukumoto SI, Yamauchi N, Moriguchi H, Hippo Y, Watanbe A, Shibahara J, Taniguichi H, Ishikawa S, Ito H, Yamamato S, Iwanari H, Horonaka M, Ishikawa H, Niki T, Sohara Y, Kodama T, Mishimura M, Fukayama M, Doska-Akita H, Auratani H. Overexpression of the aldo-keto reductase family protein AKR1B10 is highly correlated with smokers non-small cell lung carcinoma. Clin Cancer Res. 2005; 11:1776–1785. [PubMed: 15755999]
53. Gumus ZH, Du B, Kacker A, Boyle JO, Bocker JM, Mukherjee P, Subbaramaiah K, Dannenberg AJ, Weinstein H. Effects of tobacco smoke on gene expression and cellular pathways in a cellular model of oral leukoplakia. Cancer Prev Res. 2008; 1:100–111.
54. Zhang L, Lee JJ, Tang H, Fan YH, Xiao L, Ren H, Kurie J, Morcie RC, Hong WK, Mao L. Impact of smoking cessation on global gene expression in the bronchial epithelium of chronic smokers. Cancer Prev Res. 2008; 1:112–8.
55. Bolton JL, Thatcher GR. Potential mechanisms of estrogen quinone carcinogenesis. Chem Res Toxicol. 2008; 21:93–101. [PubMed: 18052105]
56. Penning TM, Burczynski ME, Hung CF, McCoull KD, Palackal NT, Tsuruda LS. Dihydrodiol dehydrogenases and polycyclic aromatic hydrocarbon activation: generation of reactive and redox-active o-quinones. Chem Res Toxicol. 1999; 12:1–18. [PubMed: 9894013]
57. Chandrasena RE, Edirisinghe PD, Bolton JL, Thatcher GR. Problematic detoxification of estrogen quinones by NAD(P)H-dependent quinone oxidoreductase and glutathione-S-transferase. Chem Res Toxicol. 2008; 21:1324–9. [PubMed: 18588320]

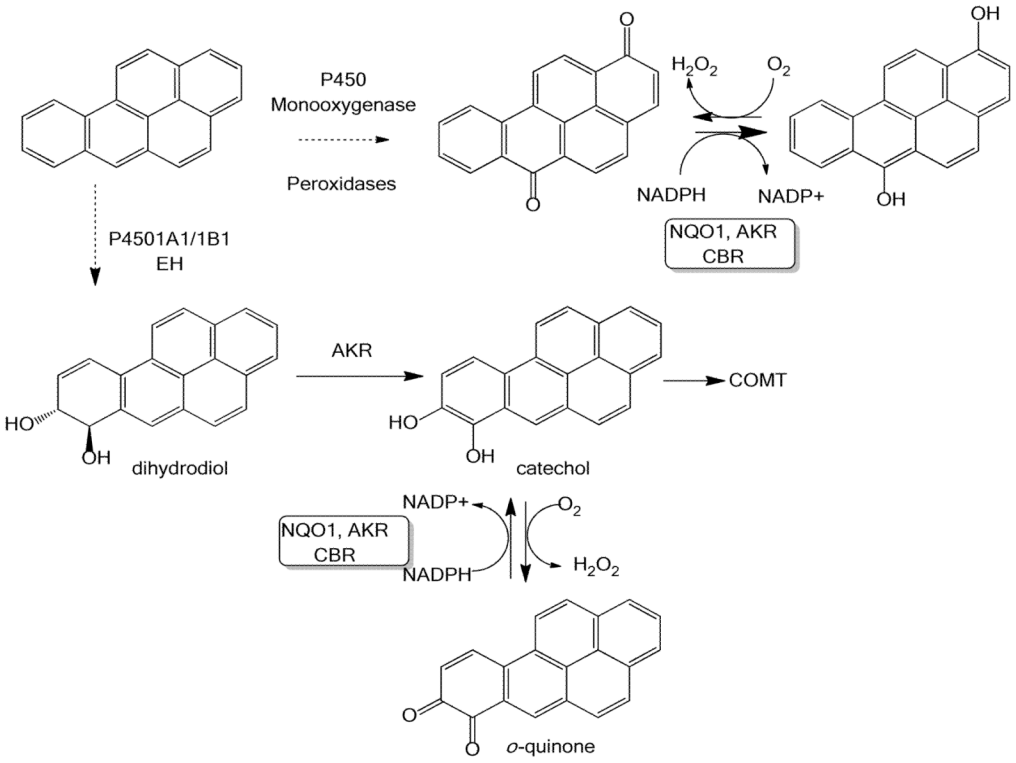

Figure 1.
Metabolic activation of B[*a*]P, a representative PAH, to dicarbonyls and the potential roles of AKRs, NQO1 and CBR1 and CBR3 in redox cycling.

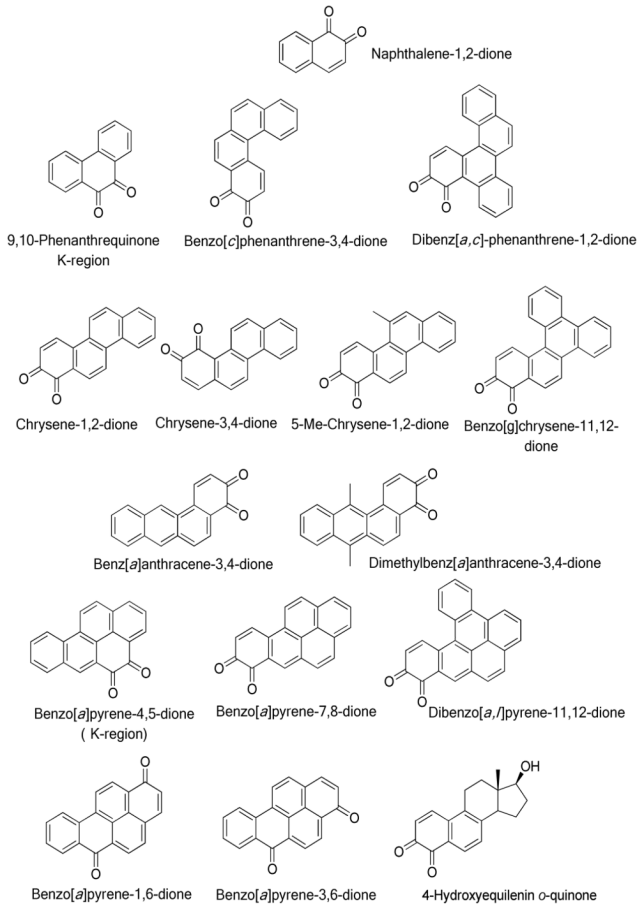

Figure 2.

Structures of quinones examined as substrates for AKRs, NQO1 and CBRs. Benzo[*a*]pyrene-1,6-dione, and benzo[*a*]pyrene-3,6-dione are remote quinones. In PAH where there are more than two fused rings and a dicarbonyl is on the terminal benzo-ring the compound is referred to as a non-K-region PAH *o*-quinone. The K-region *o*-quinones of phenanthrene and benzo[*a*]pyrene are depicted.

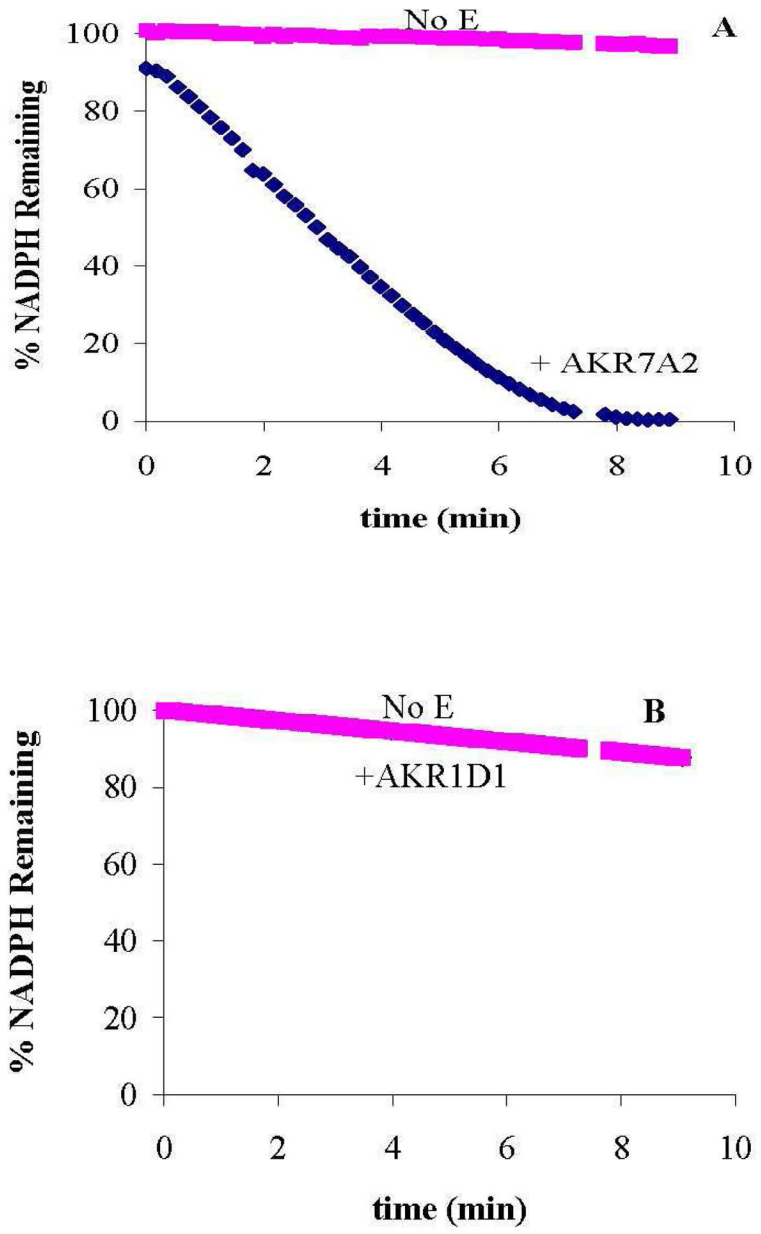

Figure 3.

NADPH consumption during the enzymatic reduction of B[*a*]P-7,8-dione catalyzed by AKR7A2. (A) Progress curve showing consumption of NADPH during quinone reduction of 10 μM B[*a*]P-7,8-dione in the presence (◆) and absence (■) of 5 μg AKR7A2 in 10 mM potassium phosphate buffer, pH 7.0, at 37° C. Reaction progress was monitored spectrophotometrically by measuring the consumption of NADPH at 340 nm. The rate of AKR7A2-mediated quinone reduction occurs at a rate much higher than rate of non-enzymatic reduction. (B) Progress curve showing NADPH consumption during the reduction of 10 μM B[*a*]P-7,8-dione observed in the presence and absence of 12 μg AKR1D1. The two rates are superimposed.

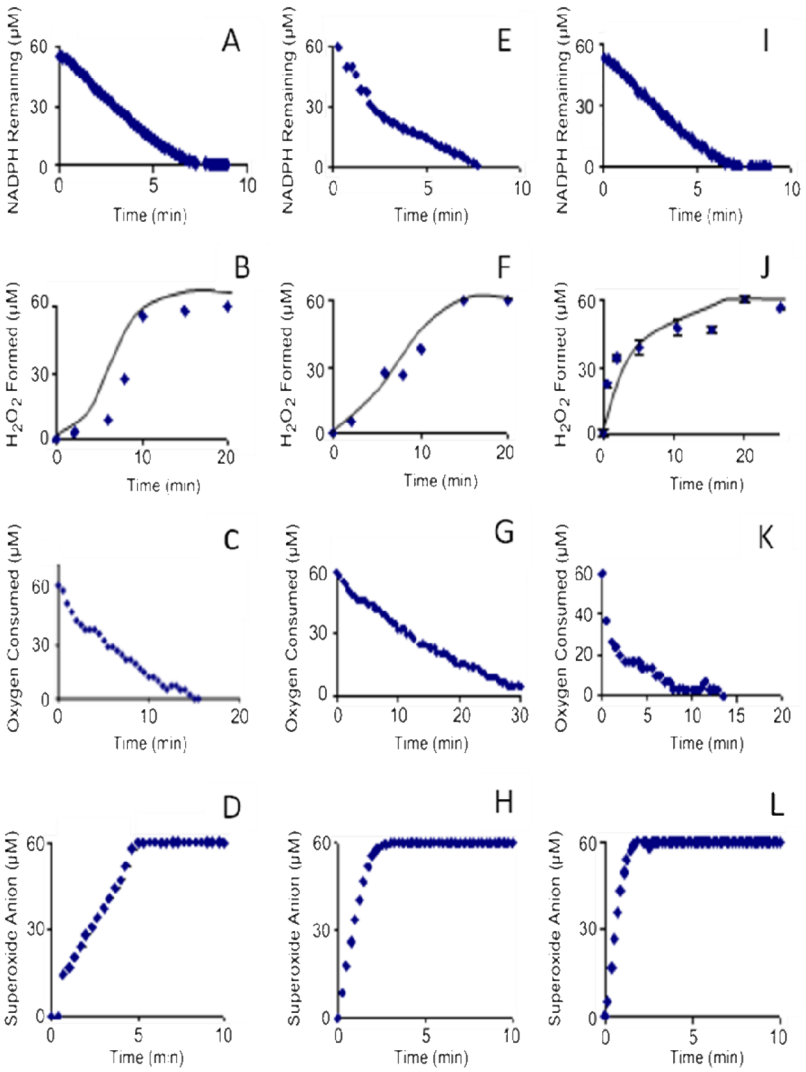

Figure 4.

The enzymatic reduction of representative quinones by AKR7A2 and AKR1C3 is accompanied by the consumption of NADPH and O_2 and the formation of H_2O_2 and superoxide anion. NADPH consumption (A), H_2O_2 formation (B), oxygen consumption (C) and superoxide anion (D) formation, during the redox-cycling of 10 μM B[*a*]P-7,8-dione catalyzed by AKR7A2. NADPH consumption (E), H_2O_2 formation (F), oxygen consumption (G) and superoxide anion (H) formation, during the redox-cycling of 10 μM B[*a*]P-3,6-dione catalyzed by AKR1C3. NADPH consumption (I), H_2O_2 formation (J), oxygen consumption (K) and superoxide anion (L) formation, during the redox-cycling of 10 μM 4-OHEN-*o*-quinone catalyzed by AKR7A2. See Materials and Methods for details.

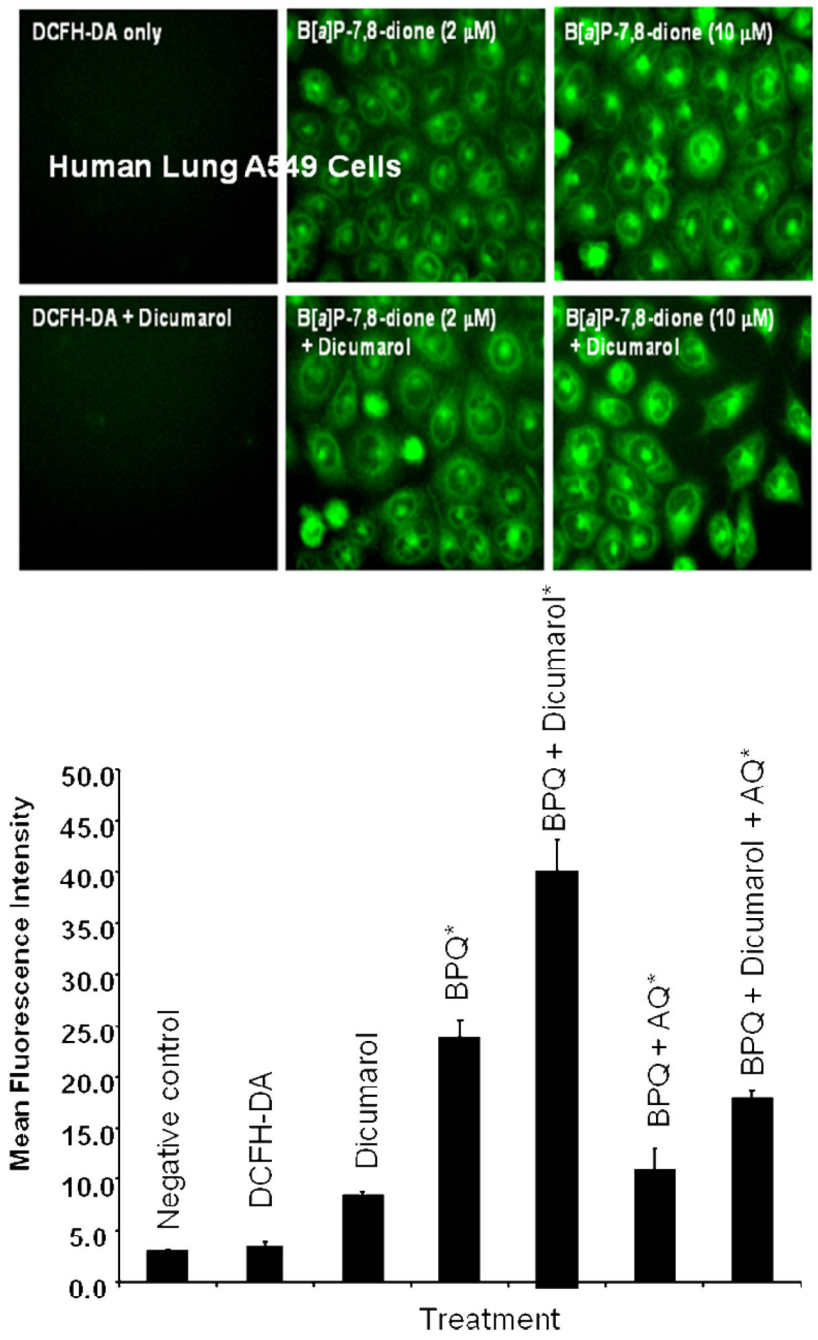

Figure 5.

B[*a*]P-7,8-dione mediated intracellular ROS formation in A549 cells is unaffected by dicumarol. Top Panel : DCFH-DA-pretreated A549 cells were incubated with 2 μM B[*a*]P-7,8-dione for 6 h in the absence and presence of 20 μM dicumarol to block potential quinone reduction by NQO1. Bottom Panel, ROS formation-mediated by B[*a*]P-7,8-dione in A549 cells as measured by FACS analysis Each experiment was performed in triplicate with the mean and standard deviation shown. Significant changes in ROS formation from the dicumarol control are denoted by * ($p < 0.050$). ROS formation in A549 cells is observed only with B[*a*]P-7,8-dione (BPQ) treatment. ROS formation is unaffected by treatment with

dicumarol. ROS formation was blocked with a mixture of antioxidants (AQ) (1 mM desferal and 250 μM α-tocopherol).

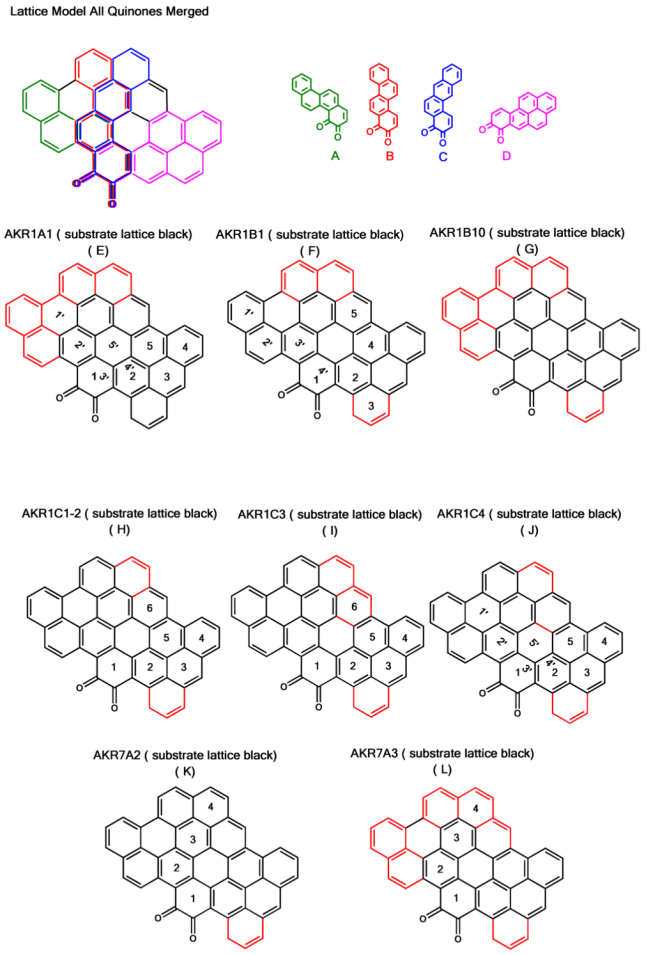

Figure 6.

Lattice structures of PAH *o*-quinones to explain substrate preference of human AKRs. Top panel, shows four different binding poses for quinones represented by the structures of C-3,4-dione (A), C-1,2-dione (B), BA-3,4-dione (C) and B[*a*]P-7,8-dione (D). The common feature is the position of the dicarbonyl which is anchored in the oxyanion hole of the AKR active site and is used for superimposition. To account for differences in substrate specificity it is assumed that: the rings in B[*a*]P-4,5-dione will overlap with those of C-1,2-dione (B); that the rings of DMBA-3,4-dione will overlap those of BA-3,4-dione (C); and that the rings of DB[*a*,*l*]P-11,12-dione, B[*g*]C-3,4-dione and DB[*a*,*c*]Ph-3,4-dione will overlap those of B[*a*]P-7,8-dione (D). The four structures are merged to give the lattice structure top left which shows the space that would be occupied at an AKR active site if all quinones were accepted (included). In the proposed lattice structures that follow (E-L) the quinone structures have been merged to account for the observed substrate specificity of the designated AKR isoform. The fused black rings account for all the PAH *o*-quinones that are substrates for a particular AKR isoform. The red rings correspond to portions of PAH *o*-quinones that are not substrates for the AKR isoform and represent disallowed (excluded) binding positions. The lattice structures are shown for AKR1A1 (E), AKR1B1 (F), AKR1B10 (G), AKR1C1-2 (H); AKR1C3 (I); AKR1C4 (J), AKR7A2 (K) and AKR7A3 (L), see text for detail.

Table 1

Substrate Specificity of Recombinant Rat AKR1C9 for PAH Quinones

Substrate	Specific Activity nmoles/min/mg
Naphthalene	
NP-1,2-dione	5,620
Phenanthrenes	
B[*c*]Ph-3,4-dione	1260
D[*a*,*c*]Ph-3,4-dione	ND
Ph-9,10-dione	5,740
Anthracenes	
BA-3,4-dione	ND
DMBA-3,4-dione	300
Equine Estrogen	
4-OHEN-*o*-quinone	180
Chrysenes	
C-1,2-dione	1,120
C-3,4-dione	410
MC-1,2-dione	650
B[*g*]C-11,12-dione	5,320
Benzo[*a*]pyrene	
B[*a*]P-7,8-dione	4,750
B[*a*]P-4,5-dione	ND
B[*a*]P-1,6-dione	ND
B[*a*]P-3,6-dione	ND
B[*a*]P-6,12-dione	25
DB[*a*,*l*]P-11,12-dione	1,360

Reactions contained 10 μM quinone and 180 μM NADPH in 10 mM potassium phosphate buffer, pH 7.0, at 37 °C. Six replicates were performed and the standard error was less than 10% of the mean value. ND = not detected; Limit of detection = 160 pmoles/min.

Table 2

Comparison of the Dihydrodiol Dehydrogenase and Quinone Reductase Activities of AKRs Using B[*a*]P Metabolites

AKR	B[*a*]P-7,8-Dihydrodiol	B[*a*]P-7,8-dihydrodiol Oxidation (nmoles/min/mg)	B[*a*]P-7.8-dione Reduction (nmoles/min/mg)
AKR1A1	(−)	16.0**	350
AKR1B1	(+)	0.13**	250
AKR1B10	(+)	0.15**	250
AKR1C1	(+/−)	3.6**	64
AKR1C2	(+/−)	4.7**	350
AKR1C3	(+/−)	0.44**	130
AKR1C4	(+/−)	2.0**	130
AKR7A2	(+/−)	ND	1270
AKR7A3	(+/−)	ND	1170

Oxidation reactions contained 20 μM B[*a*]P-7,8-dihydrodiol and 2.3 mM $NADP^+$ were measured in 50 mM MOPS buffer pH 7.4 0 at 37 °C.

** Values taken from Quinn et al.(2008a, 2008b)

Reduction reactions contained 180 μM NADPH and 10 μM B[*a*]P-7,8-dione in 10 mM potassium phosphate buffer, pH 7.0, and were performed at 37 °C. Six replicates were performed and the standard error was less than 10% of the mean value. ND = not detected. LOD = 160 pmoles/min.

Table 3

Heat Maps for Quinone Reductase Activity of AKRs

PAH	AKR1A1	AKR1B1	AKR1B10	AKR1C1	AKR1C2	AKR1C3	AKR1C4	AKR7A2	AKR7A3
NPQ	ND	260	250	ND	80	400	ND	1970	1560
9,10-PQ	79	1010	730	310	1590	1570	84	18200	8480
B[*c*]Ph-3,4-dione	170	78	160	140	78	19	ND	240	ND
DBPh-3,4-dione	32	ND	ND	ND	ND	0	ND	ND	ND
C-1,2-dione	ND	80	23	77	78	26	77	220	ND
C-3,4-dione	ND	140	ND	66	24	62	63	250	ND
MC-1,2-dione	20	78	110	100	83	130	ND	110	171
B[*g*]C-11,12-dione	370	350	440	220	370	540	64	410	ND
B[*a*]P-1,6-dione	22	ND	28	25	20	150	ND	24	31
B[*a*]P-3,6-dione	16	ND	56	41	51	150	ND	26	ND
B[*a*]P-7,8-dione	650	250	250	64	350	130	130	1270	1170
B[*a*]P-4,5-dione	ND	100	190	330	610	1260	140	990	2310
DB[*a,l*]P-11,12-dione	82	330	63	1500	510	45	61	820	77
BA-3,4-dione	ND	ND	ND	ND	ND	7	ND	130	0
DMBA-3,4-dione	ND	ND	ND	ND	ND	ND	ND	130	ND

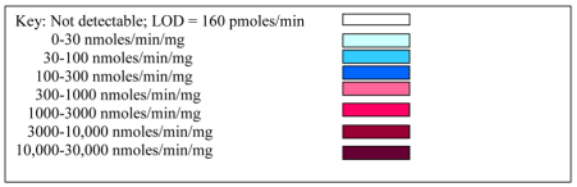

Table 4

Substrate Specificity of Human AKRs for 4-Hydroxyequilenin

Enzyme	Specific Activity (nmoles/min/mg)
AKR1A1	ND
AKR1B1	72
AKR1B10	ND
AKR1C1	5.3
AKR1C2	11.4
AKR1C3	49
AKR1C4	ND
AKR1D1	ND
AKR7A2	177
AKR7A3	5.0

Reduction reactions contained 180 μM NADPH and 10 μM 4-OHEN-*o*-quinone in 10 mM potassium phosphate buffer, pH 7.0, and were performed at 37 °C. Six replicates were performed and the standard error was less than 10% of the mean value. ND = not detected. LOD = 160 pmoles/min

Table 5

Comparison of Quinone Reductase Activity of NQO1, AKR7A2, CBR1 and CBR3

Substrate	Specific Activity (nmoles/min/mg)			
	NQO1	AKR7A2	CBR1	CBR2
Naphthalene				
NP-1,2-dione	7,260	170	830	120
Phenanthrenes				
Ph-9,10-dione	188,000	18,200	6140	250
B[*c*]Ph-3,4-dione	5,810	240	ND	ND
DB[*a*,*c*]Ph-3,4-dione	ND	ND	ND	ND
Chrysenes				
C-1,2-dione	1,470	220	130	ND
C-3,4-dione	750	260	ND	ND
MC-1,2-dione	1,950	240	ND	ND
B[*g*]C-11,12-dione	4,440	32	350	110
Anthracenes				
BA-3,4-dione	830	130	ND	ND
DMBA-3,4-dione	ND	130	ND	ND
Benzo[*a*]pyrenes				
B[*a*]P-7,8-dione	1,070	1270	ND	ND
B[*a*]P-4,5-dione	5,850	990	4620	
B[*a*]P-1,6-dione	1,990	24		
B[*a*]P-3,6-dione	40,810	26		
DB[*a*,*l*]P-11,12-dione	660	820	510	ND
Equine Estrogen				
4-OHEN-*o*-quinone	18,400	177	ND	ND

Reduction reactions contained 180 μM NADPH in 10 mM potassium phosphate buffer, pH 7.0, and were performed at 37 °C. Six replicates were performed and the standard error was less than 10% of the mean value. ND = not detected. LOD = 160 pmoles/min